*Bull. Mater. Sci.* (2020) 43:48
https://doi.org/10.1007/s12034-019-2020-0


# Time-resolved fluorescence decay and Gaussian analysis of P3HT-derived $Ho^{3+}$- and $Tm^{3+}$-doped ZnO nanostructures

**G L KABONGO[1,2,3,4], P S MBULE[1], G H MHLONGO[2], B M MOTHUDI[1] and M S DHLAMINI[1,*]**
[1]Department of Physics, University of South Africa, P.O. Box 392, Pretoria 0003, South Africa
[2]CSIR-National Centre for Nano-structured Materials, P.O. Box 395, Pretoria 0001, South Africa
[3]Département de Physique, Université Pédagogique Nationale, 8815 Kinshasa, Democratic Republic of the Congo
[4]*Present address:* TS&BHP S.E.N.C., J3B 6X4 Saint-Jean-sur-Richelieu, QC, Canada
*Author for correspondence (dhlamms@unisa.ac.za)

MS received 7 June 2019; accepted 13 September 2019

**Abstract.** The fluorescence vibrational features of as-synthesized P3HT–ZnO:$Ho^{3+}$ and P3HT–ZnO:$Tm^{3+}$ thin films were investigated using Gaussian analysis. Relative to P3HT–ZnO:$Tm^{3+}$ film, detailed Gaussian analysis of the fluorescence spectra revealed weaker intensity exhibited in P3HT–ZnO:$Ho^{3+}$ film due to better charge transfer. Moreover, we comparatively present the Huang–Rhys factor and relaxation energy of the samples, which are calculated using relations derived from the Franck–Condon theory. Furthermore, P3HT–ZnO:$Ho^{3+}$ film exhibits lower relaxation energy as compared with P3HT–ZnO:$Tm^{3+}$ film, which implies better conjugation length. Finally, the singlet exciton lifetime of P3HT–ZnO:$Ho^{3+}$ sample was found to be shorter as compared with P3HT–ZnO:$Tm^{3+}$, while the calculated exciton diffusion length was 6.4 and 10.3 nm, respectively.

**Keywords.** Exciton; P3HT; holmium; thulium; charge transfer; PL.

## 1. Introduction

Organic semiconductors, along with their puzzling fundamental properties, are nowadays the main focus of cutting-edge research worldwide [1,2]. Among the wide family of organic semiconductors, regioregular poly(3-hexylthiophene) (P3HT) has attracted interest in various technological applications owing to the maturity of its research and development as compared with its counterparts [3–5].

In recent years, considerable progress has been made in understanding the photophysical properties of P3HT, which opens up new perspectives for further research [6–8]. Spano [9] has proposed a model to describe the photoexcited state in P3HT and Clark *et al* [10] established the dominance of H-aggregate on the optical emission in regioregular P3HT. In addition, Paquin *et al* [11] have comprehensively described the photoluminescence (PL) line shape of an isolated molecule as a function of the Huang–Rhys (HR) factor, which accounts for the number of phonons involved in the relaxation process. On the other hand, several groups worked to establish that the Franck–Condon (F–C) progression appears to give the most appropriate description of the fluorescence emission of P3HT [12–15]. Conversely, other groups attempted to describe the fluorescence of P3HT using the simple Gaussian function with satisfactory output [16–19].

It turns out that one of the fundamental drawbacks of organic-based solar cells as compared with inorganics is that instead of creating free charge carriers upon photon absorption, a bound exciton is created. The electron–hole pair attraction in inorganic semiconductors is lower than the thermal energy ($kT \sim 0.025$ eV), which facilitate the generation of free charge carriers without need of additional driving force. However, in organic semiconductors, there is a need of additional energy to split the exciton into free charges. The additional energy required is the energy offset between the lowest unoccupied molecular orbitals (LUMOs) of the donor and the acceptor materials. Also known as the energetic driving force, this energy offset must overcome the exciton binding energy of P3HT, which falls in the range of ~0.1–0.4 eV. It has been widely and extensively demonstrated that the use of semiconductor nanocrystals as electron acceptor improves the photovoltaic performance mainly by increasing the charge mobility within the hybrid heterostructure [3]. Moreover, the annealing process has proven its utility in improving charge transfer from the organic donor and the inorganic acceptor [4]. In the current study we demonstrate that widening the band-gap of ZnO leads to the increase of the interfacial energetic driving force, which results in accelerating the electron transfer from P3HT to ZnO at the heterojunction interface, resulting in shortening the singlet exciton lifetime. It is worth noting that the concept of energetic driving force has not been intensively exploited as an important factor in improving the performance of hybrid heterostructures and/or photovoltaic solar cells [20,21].

Based on a wide and detailed literature analysis, it has been established that there is a need of intensive investigation in

Published online: 20 January 2020

order to elucidate the factors altering photophysical characteristic related to the fluorescent emission of P3HT. None of the reports found in the literature focused their fluorescence investigations on P3HT–ZnO:$Ho^{3+}$ and P3HT–ZnO:$Tm^{3+}$ heterostructures. Moreover, lanthanides ions such as $Ho^{3+}$ and $Tm^{3+}$ are predicted to be good candidates for optoelectronic applications, especially due to their up-conversion characteristics [22,23]. In this study, the fluorescence spectra of P3HT-based heterostructures are successfully analysed by a simple Gaussian function. The investigation aims at understanding comparatively the changes occurring in the photophysical parameters in P3HT heterostructure modified with ZnO:$Ho^{3+}$ and ZnO:$Tm^{3+}$ nanostructures. We also show that time-resolved fluorescence analysis correlates with the quenching observation revealed through PL measurements.

## 2. Experimental and theoretical considerations

The heterostructure materials under investigation have been synthesized following the method described in our previous work [8]. The room temperature (RT) PL spectra were collected using a Jobin-Yvon Fluorolog 3 spectrofluorometer. Raman scattering was measured using a HORIBA Jobin-Yvon HR800 Raman spectrometer equipped with a visible microscope and a 514 nm excitation $Ar^+$ laser with a spectral resolution of 0.4 $cm^{-1}$ at RT. Finally, the time-resolved fluorescence measurements were performed by time-correlated single-photon counting (TCSPC) technique, using a Fluoro-Hub (HORIBA Scientific, Jobin-Yvon). The samples were excited using a 455 nm NanoLED (HORIBA Scientific, Jobin-Yvon) source with a repetition rate of 1 MHz and a nominal power of 7 pJ.

The F–C model has been developed in order to overcome the limitation encountered with the Gaussian and Lorentzian model, in which the dynamic effect is neglected in the description of vibrationally resolved electronic spectra [24–26]. Moreover, the F–C model is a good derived Gaussian approximation to investigate the intensities of transitions between two vibronic states. During the past decade, several groups have successfully implemented the F–C approximation to analyse optical features of conjugated polymers [10,13,19]. Recently, the fluorescence spectra have been accurately analysed using a modified F–C progression that takes into account the H-aggregate character of the P3HT emission [10,11]:

$$I(\omega) \propto (\hbar\omega)^3 n^3(\omega) e^{-\lambda_{\text{eff}}^2} \left[ \alpha \Gamma(\hbar\omega - E_0) + \sum_{m=1,2,\ldots} \frac{\lambda_{\text{eff}}^{2m}}{m!} \alpha \Gamma(\hbar\omega - E_0 - m\hbar\Omega_0) \right] \quad (1)$$

where $n(\omega)$ is the refractive index at the optical frequency $\omega$, $\lambda_{\text{eff}}^2$ is the effective HR factor, $E_0$ is the energy of the origin of the vibronic progression, $\hbar\Omega_0 = 180$ meV is the energy of the effective oscillator coupled to the electronic transition and $\Gamma(x)$ is the *Gaussian* function that represents the homogeneously broadened spectral line of the vibronic replica in the progression. The $\alpha$-factor is a measure of the relative intensity of the origin of the vibronic progression (0–0); $\alpha$ is dissociated from the entire progression because it defines the spatial coherence of the emitting Frenkel exciton within the H-aggregate model [11,12]. However, we have analysed the fluorescence features as detected from PL measurements in our samples *via* the simple multiple peak *Gaussian* function (equation (2)). The results of this analysis are presented in table 1.

**Table 1.** Fitted parameters of P3HT–ZnO:$Ho^{3+}$ and P3HT–ZnO:$Tm^{3+}$ films as obtained *via* Gaussian multiple peak analysis of PL spectra.

| | $Ho^{3+}$ | | | $Tm^{3+}$ | | |
|---|---|---|---|---|---|---|
| Transition | $S_{0-0}$ | $S_{0-1}$ | $S_{0-2}$ | $S_{0-0}$ | $S_{0-1}$ | $S_{0-2}$ |
| Position (nm) | 638 | 685 | 783 | 650 | 680 | 756 |
| $E$ (eV) | 1.94 | 1.81 | 1.58 | 1.91 | 1.82 | 1.64 |
| $E_0$ (eV) | | 1.94 | | | 1.91 | |
| $E_p$ (eV) | | 0.18 | | | 0.18 | |
| $S$ | | 0.316 | | | 0.597 | |
| $E_{\text{rel}}$ (eV) | | 0.057 | | | 0.108 | |

$$I_{(E)} = \sum_i h_i e^{-2\frac{(E-C_i)^2}{\omega_i^2}} \quad (2)$$

where $I_{(E)}$ is the fluorescence intensity at a photon energy $E$ and $i$ denotes the energy levels, while $h_i$, $C_i$ and $\omega_i$ are, respectively, the height, centre and width parameters associated with a single *Gaussian* peak.

The HR factor can be experimentally determined by the intensity ratio of $S_{0-2}$ and $S_{0-1}$ transitions of the fluorescence vibronic progression defined by equation (3) [11]:

$$S = 2\frac{I_{\text{Fl}}^{0-2}}{I_{\text{Fl}}^{0-1}} \quad (3)$$

where $I_{\text{Fl}}^{0-n}$ is the fluorescence intensity associated with the $S_{0-n}$ transition.

The factor $S$ is the effective measure of intra-chain exciton bandwidth equivalent to the absorption intensities ratio $A_{0-0}/A_{0-1}$ [11]. The other important parameter is relaxation energy, which is related to HR factor. It is in fact the amount of energy involved when a molecule relaxes to the lowest vibronic level of the higher electronic state (figure 1), expressed by equation (4) [19]:

$$E_{\text{rel}} = SE_{\text{p}} \quad (4)$$

where $E_{\text{p}}$ is the phonon energy (180 meV).

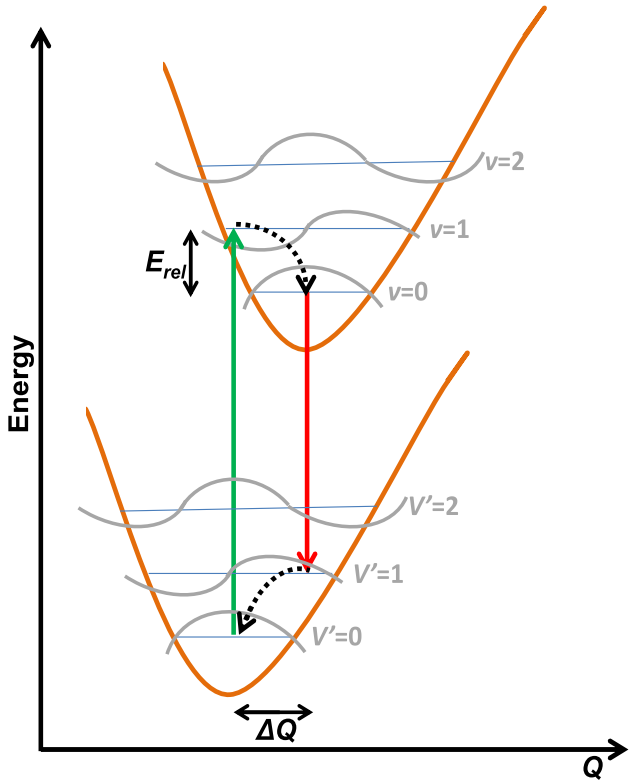


**Figure 1.** Schematic drawing of a vibronic transition in P3HT. $E_{\text{rel}}$ denotes the relaxation energy associated with 0–1 electronic transition and $Q$ represents the nuclear coordinates. Absorption associated with the transition is shown in green and fluorescence emission in red [7].

The fluorescence decay of the films has been analysed using an exponential function as presented in equation (5):

$$I(t) = I_0 \sum_{i=1}^{3} A_i e^{-(t/\tau_i)} \tag{5}$$

where $I(t)$ is the fluorescence intensity at time $t$, $I_0$ is the initial fluorescence intensity, $\tau_i$ are lifetimes and $A_i$ are pre-exponential factors.

In order to get further insight into the conformation of the films, the exciton diffusion length is derived from the one-dimensional diffusion equation for steady state presented in equation (6):

$$\frac{dn(x,t)}{dt} = D\nabla^2 n(x,t) - \frac{n(x,t)}{\tau} + g(x) = 0 \tag{6}$$

where $n(x,t)$ is the exciton density at the position $x$ and time $t$, $\tau$ is the exciton lifetime, $D$ is the diffusion constant ($D = 1.8 \times 10^{-7}$ m$^2$ s$^{-1}$) and $g(x)$ is the rate of exciton generation at the position $x$. The derived diffusion length can then be written as presented in equation (7) [27]:

$$L_{\text{D}} = \sqrt{D\tau}. \tag{7}$$

Fluorescence quenching in organic semiconductors has been previously shown to be a function of the interfacial energetic driving force, which has been defined as the energy difference between the LUMO of the donor material and the LUMO or conduction band (CB) energy level of the acceptor material [20,28]. In fact, upon creation of bound electron–hole pair (exciton) as a result of photon absorption, there is a need of energetic driving force to split the electrons and holes in order to overcome the exciton-binding energy (0.1–0.4 eV) for efficient photocurrent generation purpose [29]. The energetic driving force can be expressed by equation (8) [20]:

$$\Delta E_{\text{L-CB}} = E_{\text{L}} - (\text{IP} - E_{\text{CB}}) \tag{8}$$

where $\Delta E_{\text{L-CB}}$ is the interfacial energetic driving force, $E_{\text{L}}$ is the singlet energy of the donor, IP is the ionization potential of the donor and $E_{\text{CB}}$ is the conduction band energy level of the acceptor.

## 3. Results and discussion

Figure 2a shows the comparative PL spectra of P3HT–ZnO:$Ho^{3+}$ and P3HT–ZnO:$Tm^{3+}$ films. Considerable fluorescence intensity difference between the two samples was observed. ZnO:$Ho^{3+}$-based sample exhibited the spectrum with the lowest intensity; this is assignable to better charge transfer due to the presence of $Ho^{3+}$ ions as opposed to $Tm^{3+}$ ions. In fact, the phenomenon may result from the poor luminescence efficiency of $Ho^{3+}$ ions in the visible spectral region as compared with $Tm^{3+}$ ions [30]. It is worth noting that Chawla *et al* [28] claimed that the acceptor materials that contribute the most to lower the fluorescence intensity of P3HT are the best charge-transfer agents for P3HT-based heterostructures. Charge-transfer process and allied phenomena are closely related to

(i) the relative distance between the participating reaction centres;
(ii) the increase of the distance between the corresponding electron and hole;
(iii) the energy difference between the LUMO of the donor and the LUMO energy level of the acceptor.

Moreover, the fluorescence line shape of both P3HT-based films has been assigned to H-aggregates [6,10,12]. Elsewhere, the fluorescence quenching was associated with much faster fluorescence decay [17].

The fluorescence spectrum of P3HT–ZnO:$Ho^{3+}$, which shows two well-defined peaks, was quantitatively investigated using the Gaussian function. The spectrum was de-convoluted in a series of three individual components as shown in figure 2b. The identified peaks were found to arise from $S_{0-0}$, $S_{0-1}$ and $S_{0-2}$ transitions located at about 638, 685 and 783 nm, respectively [10,12]. The $S_{0-0}$ transition arises from

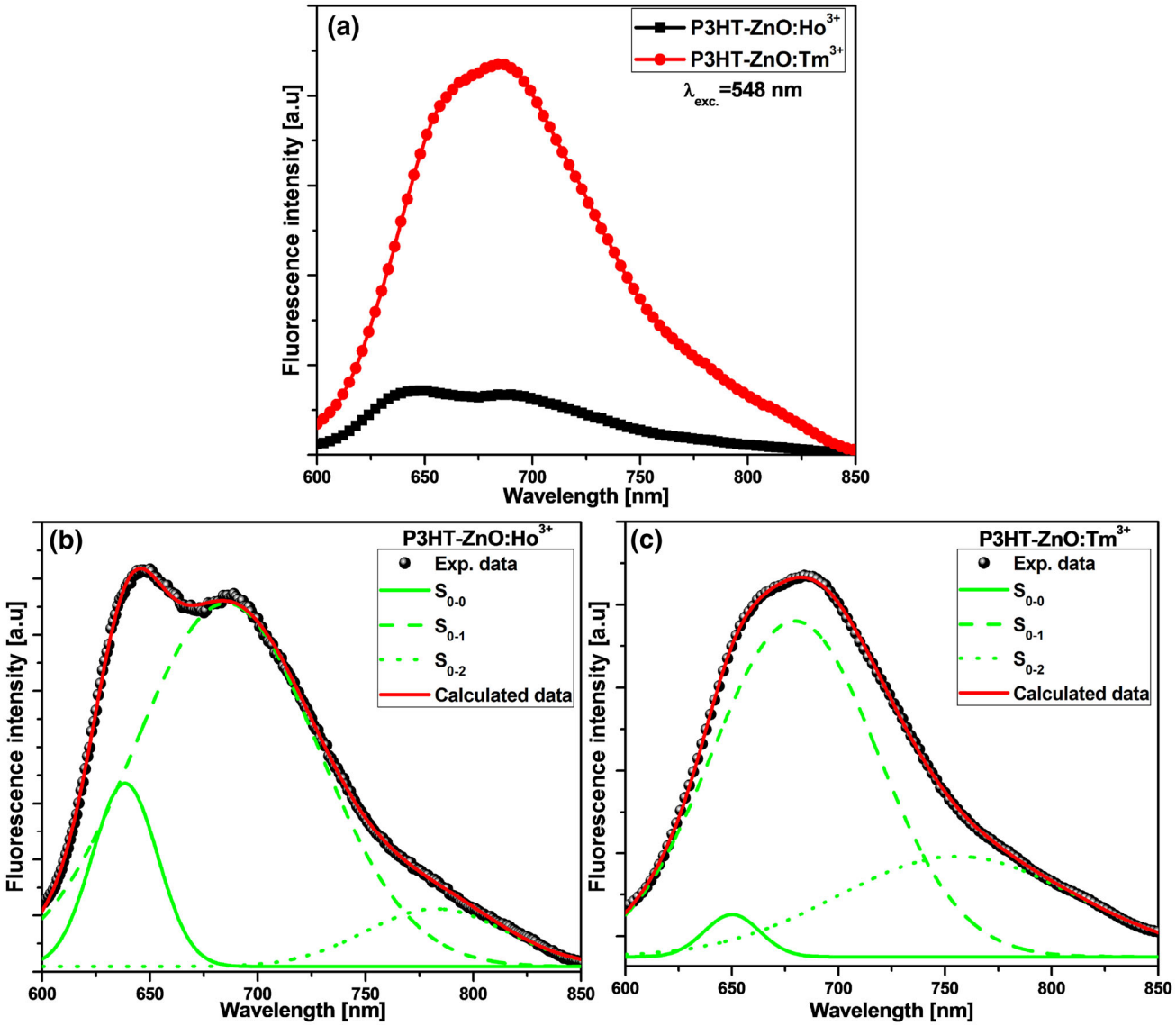


**Figure 2.** (**a**) Compared fluorescence spectra and (**b**, **c**) Gaussian de-convolution of P3HT–ZnO:$Ho^{3+}$ and P3HT–ZnO:$Tm^{3+}$ films ($\lambda_{exc} = 548$ nm).

the lowest excited state in the absence of disorder and this transition is very often not allowed [10]. However, $S_{0-1}$ and $S_{0-2}$ are sideband transitions, which are more likely to be allowed; their corresponding energies are listed in table 1 [10]. Likewise, the de-convoluted emission spectrum of P3HT–ZnO:$Tm^{3+}$ film depicted in figure 2c generated three bands located at about 650, 680 and 775 nm associated with the $S_{0-0}$, $S_{0-1}$ and $S_{0-2}$ transitions, respectively.

Interestingly, the main transition $S_{0-1}$ in the de-convoluted spectrum of P3HT–ZnO:$Ho^{3+}$ is found to be red-shifted relative to its counterpart. This band red-shift in conjugated polymer can be explained as arising from the formation of excimers, which are a bound state between ground-state chromophores and excited-state separate chromophores [31–33]. Moreover, Saidani and co-workers [13,14] recently investigated a conjugated polymer that exhibited such red-shift, which was assigned to a chain–chain contact enhancement as a result of the formation of rod-like chains of quasi coupled molecules. It is however important to mention that the high HR factor obtained for P3HT–ZnO:$Tm^{3+}$ sample implies a stronger electron–phonon interaction as compared with P3HT–ZnO:$Ho^{3+}$ sample [14]. This finding can be seen as an indication of decreased conjugation length and chain order [11]. Based on the direct proportionality of the relaxation energy *vs.* HR factor as shown in equation (3), the decrease in relaxation energy in the case of P3HT–ZnO:$Ho^{3+}$ film is found to be beneficial in improving the degree of inter-chain order of the heterostructure [19].

On the other hand, the *Lorentzian* line-shape fitting executed on the samples was found to be very poor as compared

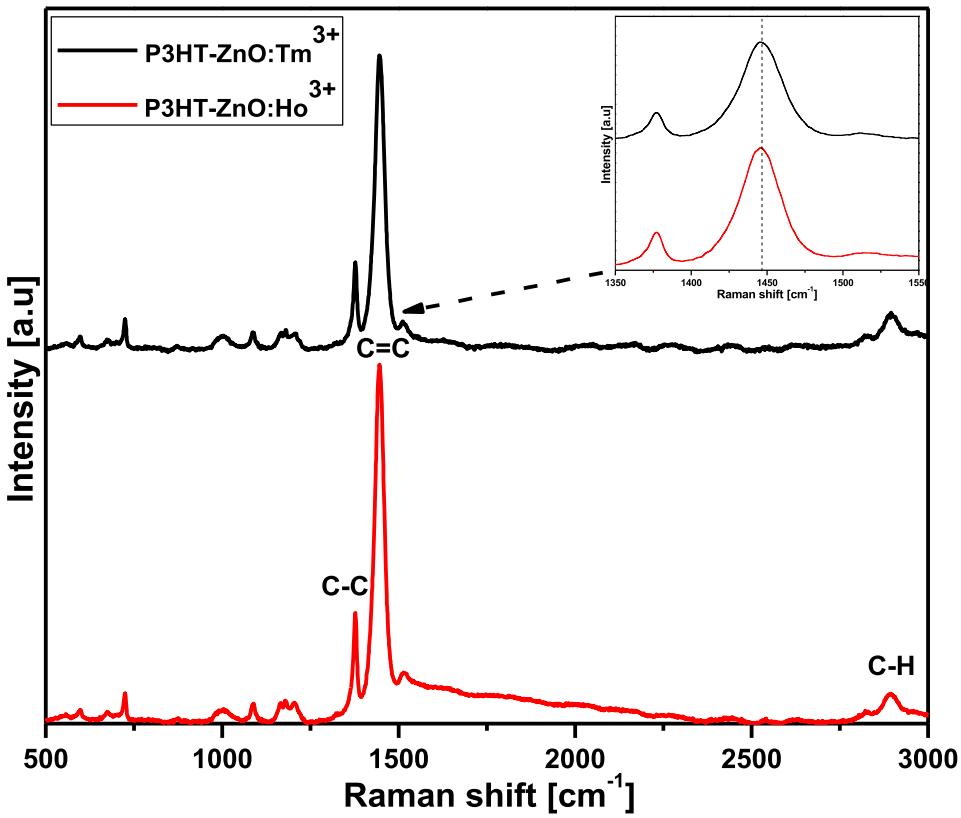


**Figure 3.** Raman spectra of P3HT–ZnO:$Ho^{3+}$ and P3HT–ZnO:$Tm^{3+}$ film.

with *Gaussian*; this is in line with the results by Brown *et al* [19], for whom features in the fluorescence spectra of conjugated polymers have a *Gaussian* line shape. It is important to note that the precise position and characteristics of the vibronic exciton features involved in fluorescence phenomena cannot be elucidated based on simple steady-state fluorescence measurements, and detailed analysis using *Gaussian* function is very useful [34].

Raman scatterings of P3HT–ZnO:$Ho^{3+}$ and P3HT–ZnO:$Tm^{3+}$ films are depicted in figure 3. The main features detected at about 1377.11, 1446.04 and 2893.91 $cm^{-1}$ were assigned to C–C in-plane skeleton vibration, the C=C stretching vibration and the C–H stretching vibration, respectively [35]. The measurements revealed that the main peak due to the C=C stretching vibration was slightly red-shifted in the $Ho^{3+}$ sample as compared with the $Tm^{3+}$ film. Finally, the $Ho^{3+}$ sample exhibits a more intense Raman scattering as compared with $Tm^{3+}$ film, which is an indication of better conjugation length and chain ordering.

One of the powerful techniques used to investigate lifetime of the excited-state is TCSPC. Figure 4 shows the fluorescence dynamics monitored at 649 nm emission in P3HT-based heterostructures under excitation at 455 nm (2.73 eV). Due to the presence of multiple de-excitation pathways in P3HT films, the decay curves were successfully fitted using exponential function from the instrument analysis software (equation (5)). The resulted average lifetimes measured for P3HT–ZnO:$Ho^{3+}$ and P3HT–ZnO:$Tm^{3+}$ films were found to be 618 and 634 ps, respectively. These obtained values are in a time scale similar to previous reports [36,37]. The observed decrease in lifetime in the P3HT–ZnO:$Ho^{3+}$ sample indicates low concentration of traps and defects, thus leading to better quality of the interface [38]. Moreover, Xu *et al* [36] investigated P3HT–$TiO_2$ nanocomposite lifetime using TCSPC technique; their findings revealed that P3HT–$TiO_2$ exhibited a fast decay as compared with P3HT. The fast decay observed in P3HT–$TiO_2$ is attributed to improved interfacial contact between P3HT and $TiO_2$, which denotes easy pathways for exciton to the heterostructure interface in order to efficiently dissociate [36,39]. Furthermore, the considerable difference in lifetime suggests that the nanostructured ZnO:$RE^{3+}$ acceptors created in the organic polymer have different environments for the excited state; this supports the previous fluorescence analysis [37]. It is worth noting that the ultrafast decay of $Ho^{3+}$ sample is closely related to the fluorescence quenching of the singlet exciton *via* efficient electron transfer; this electron transfer of photoinduced charges from donor to acceptor is highly required for efficient photovoltaic cells [40,41]. Finally, based on the lifetime, the obtained exciton diffusion length of the films as described in equation (7) is about 10.54 and 10.68 nm for P3HT–ZnO:$Ho^{3+}$ and P3HT–ZnO:$Tm^{3+}$, respectively.

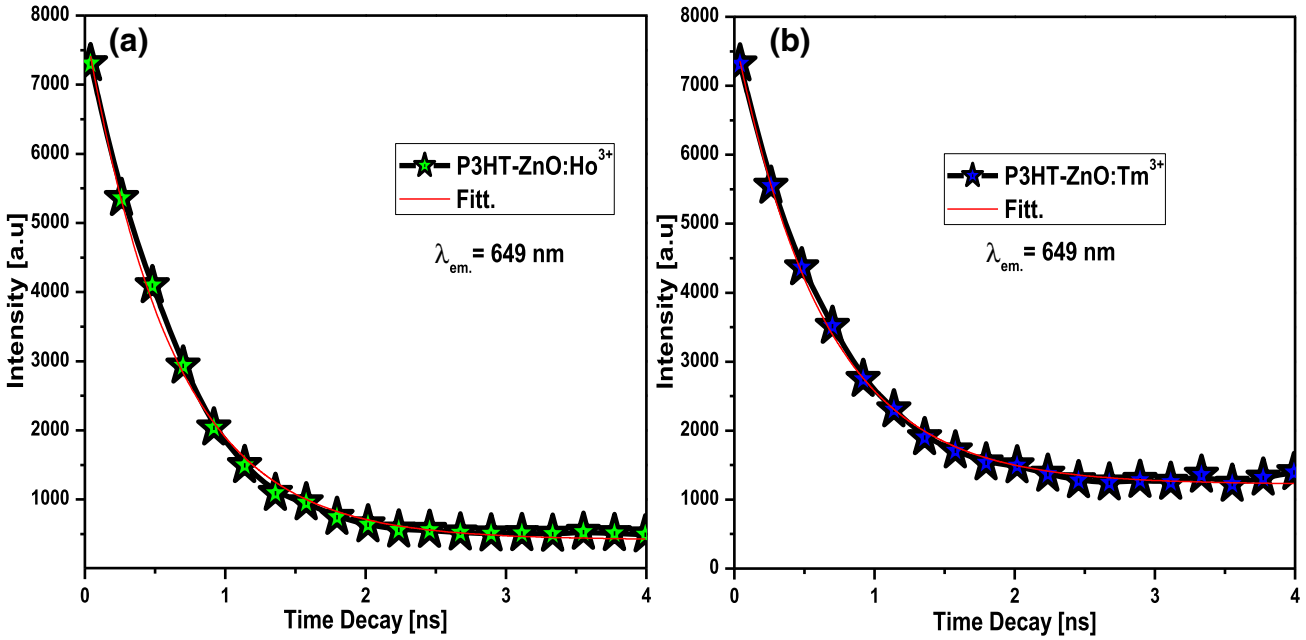


**Figure 4.** Time-resolved fluorescence decays of P3HT–ZnO:$Ho^{3+}$ and P3HT–ZnO:$Tm^{3+}$ films.

Overall, based on the results discussed earlier, we attempt to propose a model to understand the key role of exciton lifetime on efficient charge transfer in heterostructure-based P3HT–ZnO:$RE^{3+}$. It should be stressed that the primary conditions to achieve efficient charge dissociation at the heterojunction interface are the realization of a percolated network with high degree of mixture between the organic and inorganic semiconductors for better interface quality. When the heterostructure material is exposed to sunlight, the photons with energy matching the bandgap will be absorbed and further induce the creation of electron–hole pairs or excitons (process A) (figure 5a). Later, the created excitons diffuse to the heterojunction interface in order to dissociate (process B). The resulting ultrafast electron transfer process (process C), which is substantially dependent on the interfacial energetic driving force ($\Delta E_{L-CB}$) (equation (8)), paves the way for efficient charge transfer (process D) in the heterostructure [20]. Based on the fact that several reports previously ascertained the hypothesis of the dependence of electron transfer on energetic driving force, we can speculate that the shorter exciton lifetime obtained in P3HT–ZnO:$Ho^{3+}$ film as compared with P3HT–ZnO:$Tm^{3+}$ film is indicative of faster electron transfer at the heterojunction interface.

The Tauc analysis of the respective samples revealed that ZnO:$Ho^{3+}$ and ZnO:$Tm^{3+}$ nanostructures yielded bandgap values of 3.36 and 3.33 eV, respectively [8]. These values served to estimate the energetic driving force ($\Delta E_{L-CB}$) as described in equation (8); thus, $\Delta E_{L-CB}$ values of 0.56 and 0.53 eV were obtained for ZnO:$Ho^{3+}$ and ZnO:$Tm^{3+}$, respectively. It has been previously proposed that the excess energy increases the spatial separation of charges and reduces the barrier to charge separation [20]. Moreover, the charge

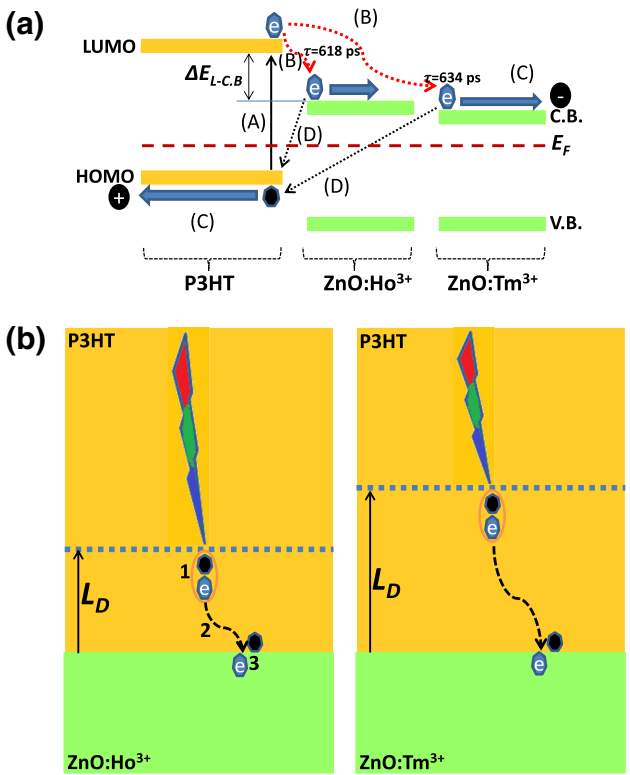


**Figure 5.** (**a**) Schematic energy diagram and (**b**) proposed exciton pathway of P3HT–ZnO:$Ho^{3+}$ and P3HT–ZnO:$Tm^{3+}$ films.

separation was found to be strongly dependent on excess energy of the photoexcited state in blends with less crystalline phase [20]. However, in the current study, the crystalline

inorganic domains are above 5 nm, which is reasonable to yield a dependence of charge separation on energetic driving force. In fact, Bansal *et al* [20] proposed a model that stressed that in organic–inorganic crystalline heterojunctions the coulomb barrier for charge separation is relatively low as compared with organic heterojunctions. Therefore, the coulomb barrier can overcome in the case where the crystalline inorganic domains are large enough to allow charge delocalization within the charge-transfer state. More precisely, when the inorganic crystallites are large enough, the coulomb binding energy is increased proportionally to the reduced charge delocalization distance, allowing the driving force to determine whether or not the charge pairs can get separated efficiently [20]. Bearing in mind that larger interfacial energetic driving force leads to larger electron transfer rate, P3HT–ZnO:$Ho^{3+}$ is a better heterostructure material for photovoltaic applications as compared with P3HT–ZnO:$Tm^{3+}$ [42]. The last but not the least assertion that could confirm the efficient charge transfer is that the short exciton diffusion length of P3HT–ZnO:$Ho^{3+}$ results from the photo-generation of excitons much closer to the donor–acceptor heterojunction interface (see figure 5b).

## 4. Conclusion

In summary, we successfully investigated the fluorescence emission of P3HT–ZnO:$Ho^{3+}$ and P3HT–ZnO:$Tm^{3+}$ by the multiple *Gaussian* peaks analysis. It has been observed that there is a considerable difference in PL intensities between the two samples, the latter exhibiting a strong emission. Additionally, P3HT–ZnO:$Ho^{3+}$ film exhibited a shorter lifetime as compared with its counterpart, while its exciton diffusion length decreased. Finally, the relaxation energy was found to increase by a factor of 1.9 in the P3HT–ZnO:$Tm^{3+}$, leading to decrease in conjugation length, hence making P3HT–ZnO:$Ho^{3+}$ film a better candidate for photovoltaic solar cell applications.

## Acknowledgements

The authors are grateful to the University of South Africa (UNISA) and National Research Foundation (NRF) (Grant# 88028) for their valuable support. They also acknowledge the financial support received from the Council for Scientific and Industrial Research (CSIR) of South Africa.

## References

[1] Thompson N J, Wilson M W B, Congreve D N, Brown P R, Scherer J M, Bischof T S *et al* 2014 *Nat. Mater.* **13** 1039
[2] Tabachnyk M, Ehrler B, Gélinas S, Böhm M L, Walker B J, Musselman K P *et al* 2014 *Nat. Mater.* **13** 1033
[3] Ntwaeaborwa O M, Zhou R, Qian L, Pitale S S, Xue J, Swart H C *et al* 2012 *Phys. B: Condens. Matter Phys.* **407** 1631
[4] Mbule P S, Kim T H, Kim B S, Swart H C and Ntwaeaborwa O M 2013 *Sol. Energy Mater. Sol. Cells* **112** 6
[5] Malgas G F, Motaung D E, Mhlongo G H, Nkosi S S, Mwakikunga B W, Govender M *et al* 2014 *Thin Solid Films* **555** 100
[6] Spano F C and Silva C 2014 *Annu. Rev. Phys. Chem.* **65** 477
[7] Paquin F 2014 *PhD thesis* (Canada: Université de Montréal)
[8] Kabongo G L, Mbule P S, Mhlongo G H, Mothudi B M, Hillie K T and Dhlamini M S 2016 *Nanoscale Res. Lett.* **11** 418
[9] Spano F C 2005 *J. Chem. Phys.* **122** 234701; Erratum 2007 *J. Chem. Phys.* **126** 159901
[10] Clark J, Silva C, Friend R H and Spano F C 2007 *Phys. Rev. Lett.* **98** 206406
[11] Paquin F, Yamagata H, Hestand N J, Sakowicz M, Berube N, Côté M *et al* 2013 *Phys. Rev. B* **88** 155202
[12] Spano F C, Clark J, Silva C and Friend R H 2009 *J. Chem. Phys.* **130** 074904
[13] Saidani M A, Benfredj A, Ben Hamed Z, Romdhane S, Ulbricht C, Egbe D A M *et al* 2013 *Synth. Met.* **184** 83
[14] Saidani M A, Benfredj A, Romdhane S, Kouki F and Bouchriha H 2012 *Phys. Rev. B* **86** 165315
[15] Ben Hamed Z, Mastour N, Ben chaabane A, Kouki F, Sanhoury M A and Bouchriha H 2016 *J. Lum.* **170** 30
[16] Li N, Shi T, Ye C, Zeng X, Li X, Zhao Y *et al* 2014 *Europhys. Lett.* **107** 28007
[17] Wang C H, Chen C W, Chen Y T, Chen C T, Chen Y F, Chou S W *et al* 2011 *Nanotechnology* **22** 065202
[18] Motaung D E, Malgas G F, Arendse C J, Mavundla S E and Knoesen D 2009 *Mater. Chem. Phys.* **116** 279
[19] Brown P J, Thomas D S, Kohler A, Wilson J S and Kim J S 2003 *Phys. Rev. B* **67** 064203
[20] Bansal N, Reynolds L X, MacLachlan A, Lutz T, Ashraf R S, Zhang W *et al* 2013 *Sci. Rep.* **3** 1531
[21] Bakulin A A, Rao A, Pavelyev V G, Van Loosdrecht P H M, Pshenichnikov M S, Niedzialek D *et al* 2012 *Science* **335** 1340
[22] Lian H, Hou Z, Shang M, Geng D, Zhang Y and Lin J 2013 *Energy* **57** 270
[23] Barone V, Bloino J and Biczysko M 2009 *Vibrationally-resolved electronic spectra in Gaussian 09* Gaussian 09, Revision A.02, http://dreamslab.sns.it [accessed, 06 January 2016]
[24] Kabongo G L, Mhlongo G H, Mothudi B M, Mbule P S, Hillie K T and Dhlamini M S 2017 *J. Lum.* **187** 141
[25] Franck J 1926 *Trans. Faraday Soc.* **21** 536
[26] Condon E 1928 *Phys. Rev.* **32** 858
[27] Shaw P E, Ruseckas A and Samuel I D W 2008 *Adv. Mater.* **20** 3516
[28] Chawla P, Singh S and Sharma S N 2014 *Beilstein J. Nanotechnol.* **5** 1235
[29] McGehee M D and Goh C 2008 *AIP Conf. Proc.* **1044** 322
[30] Bünzli J C G and Eliseeva S V 2010 in *Lanthanide luminescence: photophysical, analytical and biological aspects*, P Hanninen and H Harma (eds) Springer Series on Fluorescence, https://doi.org/10.1007/4243_2010_3
[31] Yanga K, Kumara J, Leeb D, Sandman D J and Tripathy S K 2002 *Opt. Commun.* **201** 197
[32] Yu J, Hu D and Barbara P F 2000 *Science* **289** 1327

[33] Hu D, Yu J, Wong K, Bagchi B, Rossky P J and Barbara P F 2000 *Nature* **405** 1030
[34] Grey J K, Kim D Y, Donley C L, Miller W L, Kim J S, Silva C *et al* 2006 *J. Phys. Chem. B* **110** 18898
[35] Shao M, Keum J, Chen J, He Y, Chen W, Browning J F *et al* 2014 *Nat. Commun.* **5** 4180
[36] Xu J, Wang J, Mitchell M, Mukherjee P, Jeffries E L M, Petrich J W *et al* 2007 *J. Am. Chem. Soc.* **129** 12828
[37] Chasteen S V, Carter S A and Rumbles G 2005 *Proc. SPIE* **5938** 59380J
[38] Li Y, Lu P, Jiang M, Dhakal R, Thapaliya P, Peng Z G *et al* 2012 *J. Phys. Chem. C* **116** 25248
[39] Sun B, Snaith H J, Dhoot A S, Westenhoff S Q and Greenham N C 2005 *J. Appl. Phys.* **97** 014914
[40] Goutam P J, Singh D K and Iyer P K 2012 *J. Phys. Chem. C* **116** 8196
[41] Markov D E, Amsterdam E, Blom P W M, Sieval A B and Hummelen J C 2005 *J. Phys. Chem. A* **109** 5266
[42] Zheng F, Xu W L, Jin H D, Hao X T and Ghiggino K P 2015 *RSC Adv.* **5** 89515